

# Effect of Diphenyldisulfides with Different Substituents on the Reclamation of NR Based Latex Products

V. V. Rajan,<sup>1</sup> W. K. Dierkes,<sup>1</sup> R. Joseph,<sup>2</sup> J. W. M. Noordermeer<sup>1</sup>

<sup>1</sup>Department of Rubber Technology, Faculty of Science and Technology, University of Twente, 7500 AE Enschede, The Netherlands

<sup>2</sup>Department of Polymer Science and Rubber Technology, Cochin University of Science and Technology, Kochi 22, Kerala, India

Received 21 October 2005; accepted 4 September 2006

DOI 10.1002/app.25925

Published online in Wiley InterScience (www.interscience.wiley.com).

**ABSTRACT:** The latex industry has expanded over the years to meet the world demands for gloves, condoms, latex thread etc. Because of the strict specifications for the products and the unstable nature of the latex, as high as 15% of the final latex products are rejected. Since waste latex rubber (WLR) represents a source of high quality rubber hydrocarbon, it is a potential candidate for generating reclaimed rubber of superior quality. Two types of WLR with different amounts of polysulfidic bridges are used in these experiments, which are reclaimed with variation of the concentration of the reclaiming agents, the reclamation temperature and time. Diphenyldisulfide, 2-aminophenyldisulfide and 2,2'-dibenzamidodiphenyldisulfide (DBADPDS) are used as reclaiming agents, and the effect of diphenyldisulfides (DPDS) with different substituents, on the reclamation efficiency

of WLR is investigated. A kinetic study of the reclamation reaction with the three reclaiming agents is done. The reaction rates and activation energies are calculated and compared with literature values. The comparative study of the three different reclaiming agents shows that (DBADPDS) is able to break the crosslinks at temperature levels  $\sim 20^\circ\text{C}$  below the temperature levels normally used with DPDS. Another advantage of this reclaiming agent is the reduced smell during the reclamation process and of the final reclaims, one of the most important shortcomings of other disulfides used for this purpose. © 2007 Wiley Periodicals, Inc. *J Appl Polym Sci* 104: 3562–3580, 2007

**Key words:** rubber; recycling; diphenyldisulfides; activation energy; crosslinking

## INTRODUCTION

For both environmental and economic reasons, there is a growing interest in recycling of scrap rubber and development of improved recycling technologies. The focus of recent research is to apply processes free of hazardous by-products and that might be carried out directly in the product manufacturer's factory. The most important recycling process currently is to utilize scrap rubber as a very finely ground powder, produced either by ambient temperature mechanical grinding or by cryogenic shattering. In general, the powder rubber is combined with virgin elastomer compounds to reduce the costs with the additional advantage of an improvement of the processing behavior. However, some loss in physical properties and performance is observed.

This factor has motivated the search for cost effective *in situ* regeneration or devulcanization of the scrap rubber to provide recycled material with superior

properties. It is well known that direct material recycling and reshaping is difficult because of the irreversible three-dimensional crosslinking of rubber. Countless attempts have been proposed for material-sensitive recycling of rubber.<sup>1–5</sup> Most processes are based on mechanical shear, heat, and energy input together with a combination of chemicals such as oils, accelerators, amines, or disulfides to reduce the concentration of sulfur crosslinks in the vulcanized rubber.<sup>6</sup> An alternative to mechanical energy input and direct heating is microwave treatment.<sup>7–9</sup> Destruction of the main chains accompanies all the high-temperature methods and thus leads to the partial loss of physical and mechanical properties of the reclaim.

The three dimensional network of sulfur-cured elastomers has the following types of chemical bonds

- (i) C—C, carbon–carbon bonds
- (ii) C—S—C, sulfur–carbon bonds, and
- (iii) C—S—S—C, C—S<sub>x</sub>—C ( $x \geq 3$ ), sulfur–sulfur bonds.

Correspondence to: J. W. M. Noordermeer (j.w.m.noordermeer@utwente.nl).

**TABLE I**  
**Bond Strength of Different Bonds in Rubber Network**

Type of bond	Bond dissociation energy (kJ/mol)
C—C	349
C—S—C	302
C—S—S—C	273
C—S <sub>x</sub> —C (x ≥ 3)	256

ducted by means of destruction of the interchain crossbonds such as C—S—C, C—S—S—C, as well as C—S<sub>x</sub>—C (x ≥ 3) and/or by main-chain bonds in the elastomer.<sup>10</sup>

Molecular weight reduction because of mechanical energy input results from the cleavage of polymer chains. Without chemical deactivation in a reaction with oxygen or other radical scavengers, the free radicals from the chain scission will predominately recombine. However, some chain transfer chemistry and disproportionation reactions will hasten the molecular weight reduction. As a consequence, chemical peptisers have served the rubber industry in the function of a host for radically reactive chemicals. For many years, mercaptans (especially pentachlorothiophenol) were the chemicals of choice as peptisers for natural rubber. However, toxicity issues have shifted the market to the predominant use of dibenzamidodiphenyldisulfide and other softening agents.<sup>11</sup>

Diphenyldisulfide (DPDS) is an effective reclaiming agent for NR based latex products.<sup>12</sup> In this article

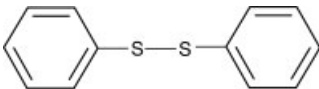
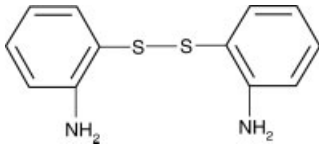
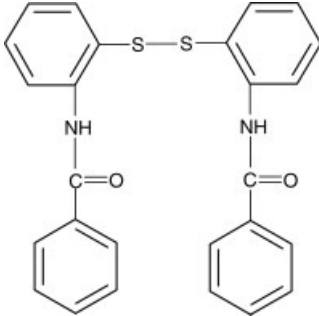
the study will be extended with different types of aromatic disulfides. It is commonly accepted that DPDS gives rise to free radicals by thermal decomposition of the S—S bond.<sup>3</sup> The dissociation energy of the S—S bond in DPDS is 225 kJ/mol. The radicals generated are able to dehydrogenate substances and the process can be divided into three steps

- (i) The homolytic decomposition of disulfides into radicals;
- (ii) Hydrogen abstraction by the benzenesulfide radical from the polymer chain, resulting in the formation of polymer radicals;
- (iii) Combination of another disulfide radical with the polymer radical to stabilize the polymer chain.

The rate determining step of the overall reaction is the first step. The time necessary for reclamation is therefore dependent on the decomposition rate of the disulfide. The efficiency of the overall reaction mainly depends on the type of radicals formed after decomposition of the disulfide and of the substrate.

In this article the effect of different substituents on the *o*-position of DPDS is investigated and their reactivity as reclaiming agent for NR based latex products is compared. This allows a view on the effect of the structure of aromatic disulfides on the efficiency of reclaiming. Three aromatic disulfides are selected: diphenyldisulfide, 2-aminophenyldisulfide (APDS),

**TABLE II**  
**Chemical Name and Structure of the Different Reclaiming Agents**

Chemical name	Chemical structure
Diphenyldisulphide, DPDS (218.34 g/mol)	
2-aminophenyldisulphide, APDS (248.37 g/mol)	
2,2'-dibenzamidodiphenyldisulphide, DBADPDS (456.57g/mol)	

**TABLE III**  
Reclaiming Recipe

Material	Amount (phr)
WLR	100
Reclaiming agent	0, 0.5, 1, 1.5, 2
Reclaiming oil	5

and 2,2'-dibenzamidodiphenyldisulfide (DBADPDS). DPDS is taken as the reference material. DBADPDS was selected, since this is used successfully as masticating agent for natural rubber,<sup>11</sup> in analogy with DPDS. APDS was selected to study the effect of the  $-\text{NH}_2$  group. DBADPDS has an additional  $\text{C}_6\text{H}_5\text{CO}-$  substituent on the amino group. The sulfur content of DPDS is 29%; the sulfur content of APDS is 26% and the sulfur content of DBADPDS is 14% of its mass. This is an important, characteristic because the amount of sulfur in the reclaiming agent influences the formation of mono- and disulfidic crosslinks during reclaiming. The higher the sulfur content in the reclaiming agent the higher is the probability of formation of mono- and disulfides.<sup>13</sup>

## EXPERIMENTAL SECTION

### Materials

The WLR used in this investigation was gloves (WLR1) and condoms (WLR2). WLR1 was obtained from Primus Gloves Pvt., Kochi, Kerala, India and WLR2 was obtained from Hindustan Latex, Thiruvananthapuram, Kerala, India. In WLR1 a mixture of Zinc diethyldithiocarbamate (ZDEC) and Zinc 2-mercaptobenzthiazolate (ZMBT) was used as accelerators; the sulfur/accelerator ratio was less than 1. In WLR2 a mixture of different dithiocarbamates was

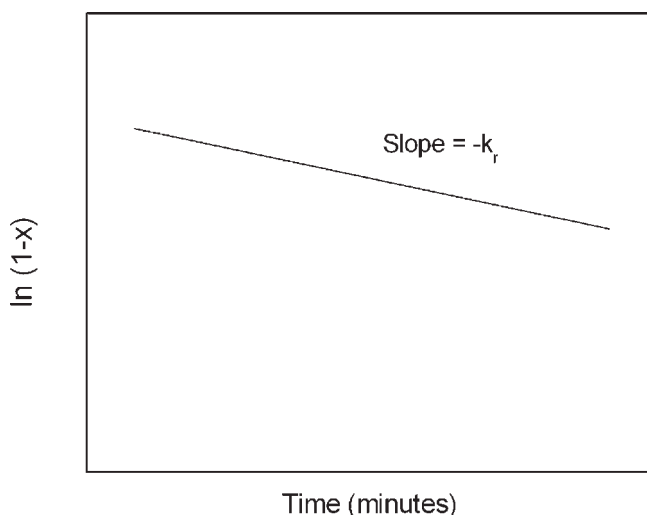


**Figure 1** Determination of reaction constant.

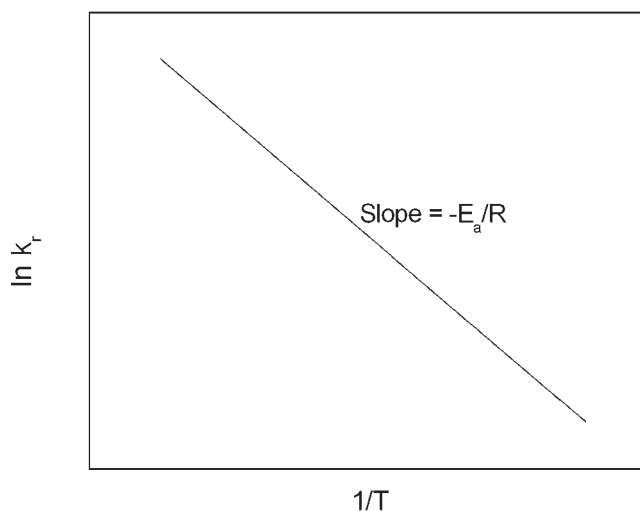


**Figure 2** The Arrhenius plot of  $\ln k_r$  versus  $1/T$ .

used as accelerator and the sulfur/accelerator ratio was higher than 1.

The reclaiming additives investigated were DPDS (Acros, 99%), APDS (Aldrich, 98%), and DBADPDS (Lancaster, 97%). The chemical name and structure of the reclaiming agents are given in Table II. Treated distillate aromatic extract, TDAE, (BP Oil) was used as reclaiming oil.

### Reclamation experiments

The feedstock was ground by passing it twice through a cold two-roll mill (Schwabenthan) with a nip size of 0.2 mm. The reclaim was prepared according to the recipe shown in Table III by a batch process in an internal mixer (Brabender Plasticorder

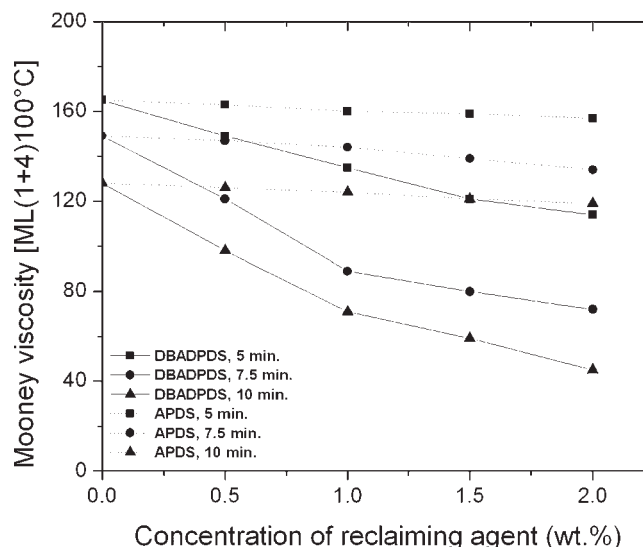


**Figure 3** Mooney viscosity as a function of concentration of DBADPDS and APDS at various times for WLR1 at 150°C.

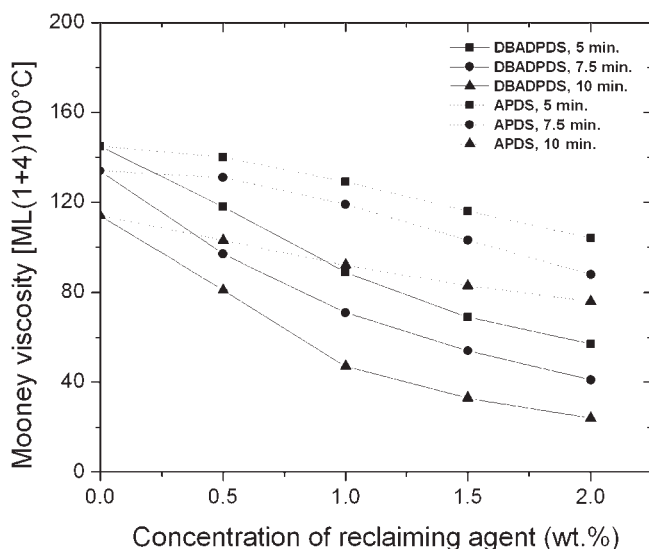


**Figure 4** Mooney viscosity as a function of concentration of DBADPDS and APDS at various times for WLR1 at 160°C.

PL-2000) having a mixing chamber volume of 50 cc and a cam-type rotor. The batch size was 30 g. A constant rotor speed of 50 rpm was applied. The reclaiming temperature was 150, 160, 170, and 180°C and reclaiming time was 5, 7.5, and 10 min. TDAE was added prior to the addition of the reclaiming agent. After reclamation, the reclaimed material was passed twice through the cold two-roll mill with a nip size of 0.2 mm to form a sheet.

### Testing procedures

The Mooney viscosity—ML (1 + 4)100°C—of the reclaim was determined using a Mooney viscometer

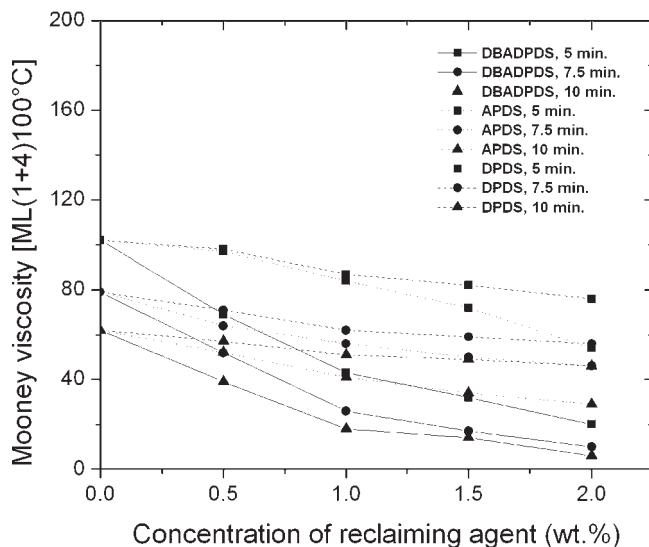


**Figure 5** Mooney viscosity as a function of concentration of DBADPDS, APDS and DPDS at various times for WLR1 at 170°C.

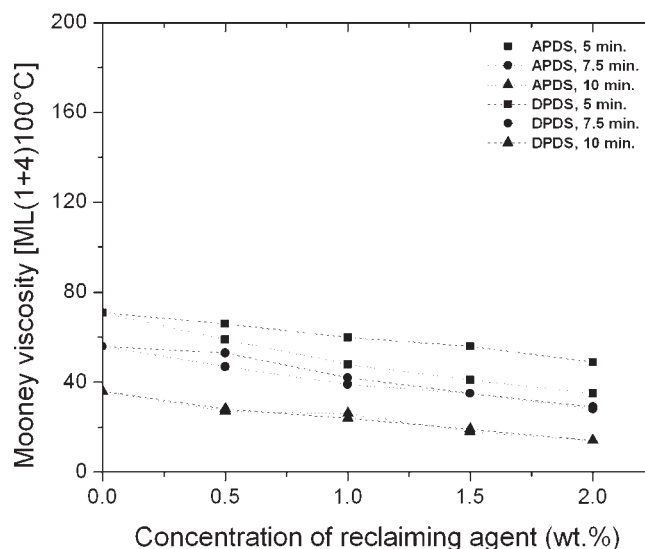


**Figure 6** Mooney viscosity as a function of concentration of APDS and DPDS at various times for WLR1 at 180°C.

(MV2000 VS) according to ISO R289. Measurements were performed directly after reclamation.

After reclamation, the reclaim was extracted in a Soxhlet apparatus, first with acetone for 48 h to extract the polar substrates, and then with tetrahydrofuran (THF) for 72 h to extract debound polymers. During the extractions the samples were kept in the dark under nitrogen atmosphere. The completion of the extraction was checked by drying the samples and determining the weight loss until no further significant amount of solubles (<0.1%) could be extracted. The sol fraction ( $S_f$ ) of reclaim was defined as the total soluble fraction (in acetone and

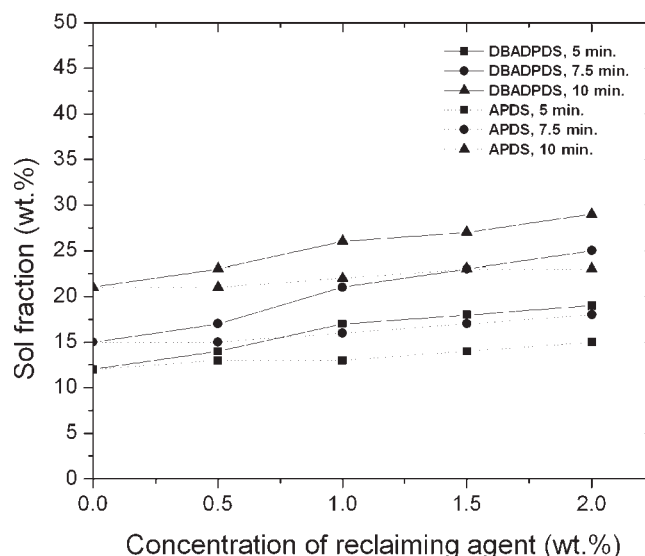


**Figure 7** Sol fraction as a function of concentration of DBADPDS and APDS at various times for WLR1 at 150°C.

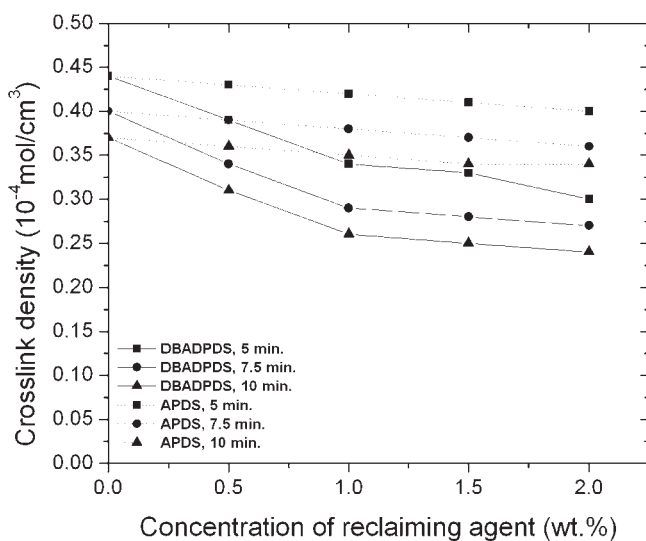


**Figure 8** Crosslink density as a function of concentration of DBADPDS and APDS at various times for WLR1 at 150°C.

THF) minus the amount of reclaiming agent and reclaiming oil added.

The elastically active network chain density was measured with equilibrium swelling in toluene for 72 h. The data were analyzed according to the Flory–Rehner equation, modified for tetra-functional networks by using swelling measurement data.<sup>14</sup>

$$v = \frac{-[\ln(1 - v_r) + v_r + \chi v_r^2]}{V_s(v_r^{1/3} - 0.5v_r)} \quad (1)$$

where  $v_r$  is the volume fraction of the polymer in the vulcanizate swollen to equilibrium,  $\chi$  is the polymer–solvent interaction parameter,  $v$  is the number

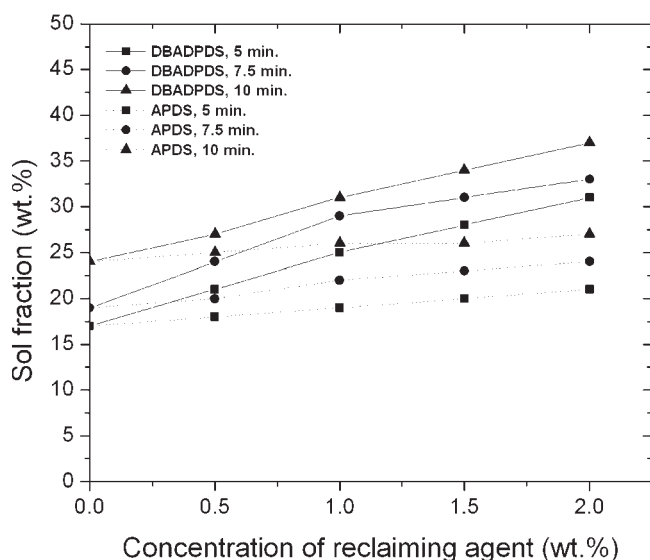


**Figure 9** Sol fraction as a function of concentration of DBADPDS and APDS at various times for WLR1 at 160°C.

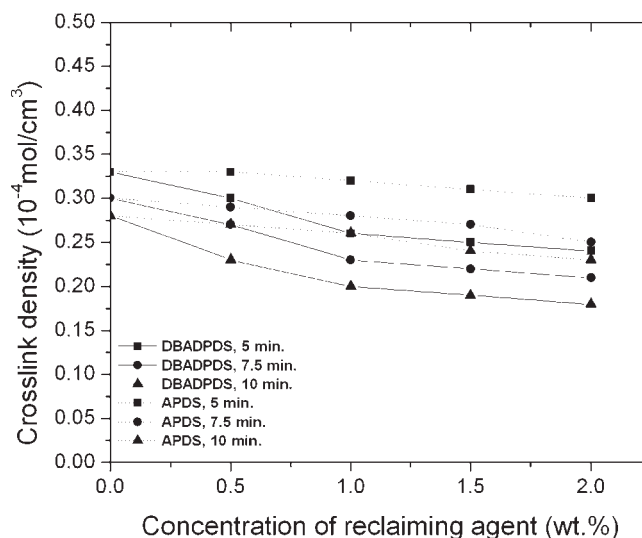


**Figure 10** Crosslink density as a function of concentration of DBADPDS and APDS at various times for WLR1 at 160°C.

of elastically active network chains per unit volume, and  $V_s$  is the solvent molar volume.

The crosslink distribution of the feedstock and the reclaim were studied using thiol/amine chemical probes.<sup>15,16</sup> Samples with known overall crosslink density were preswollen in toluene for 72 h before adding the reagents to ensure unhindered diffusion. 2-propanethiol in combination with piperidine cleaves polysulfidic crosslinks in 2 h and 1-hexanethiol with piperidine cleaves poly- and disulfidic crosslinks in 48 h. Therefore, 2-propanethiol/piperidine treatment allows the determination of the amount of monoplus disulfidic crosslinks, whereas 1-hexanethiol/pi-

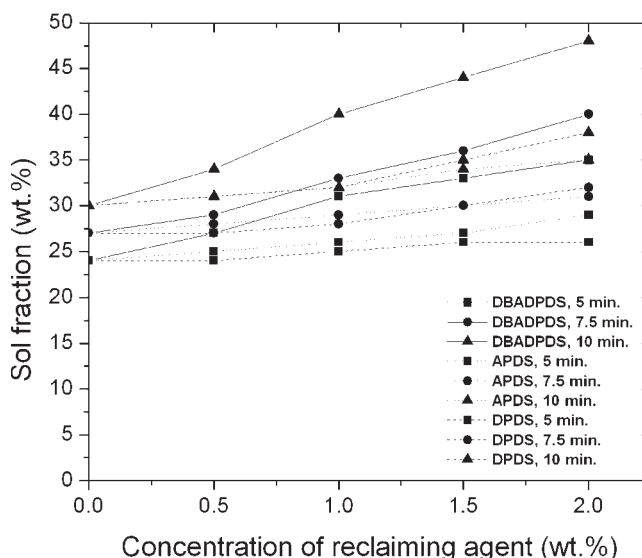


**Figure 11** Sol fraction as a function of concentration of DBADPDS, APDS, and DPDS at various times for WLR1 at 170°C.

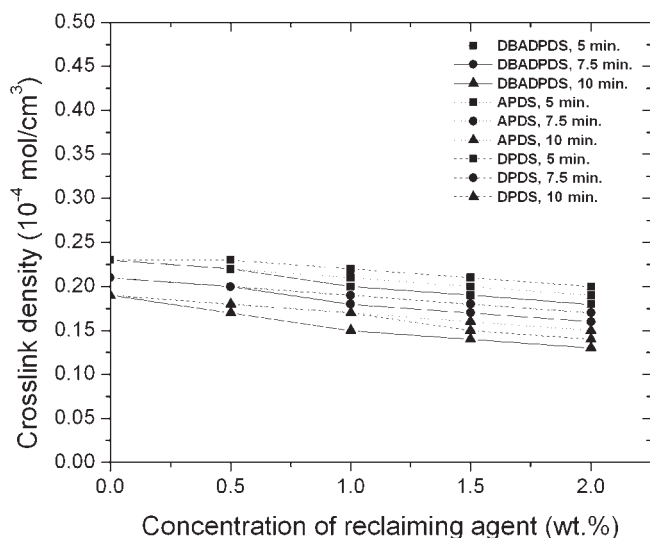


**Figure 12** Crosslink density as a function of concentration of DBADPDS, APDS, and DPDS at various times for WLR1 at 170°C.

peridine treatment gives the amount of monosulfidic crosslinks. After the chemical probe treatment, the crosslink densities of the remaining samples were measured with equilibrium swelling in toluene for 72 h, as mentioned in eq. (1). Once, the amount of monosulfidic, mono- plus disulfidic, and overall crosslink density is estimated separately, simple mathematical calculation allows the determination of mono-, di-, and polysulfidic crosslinks separately.

Molecular weight of the polymers were determined with gel permeation chromatography (GPC). Solutions of 5 mg/mL in THF were filtered over 0.45- $\mu\text{m}$  filters (Schleicher and Schuell) and analyzed with Waters styragel columns (pores  $10^5$ ,  $10^4$ ,  $10^3$ , and  $5 \times 10^2$  Å) with a flow rate of 1.47 mL/min.

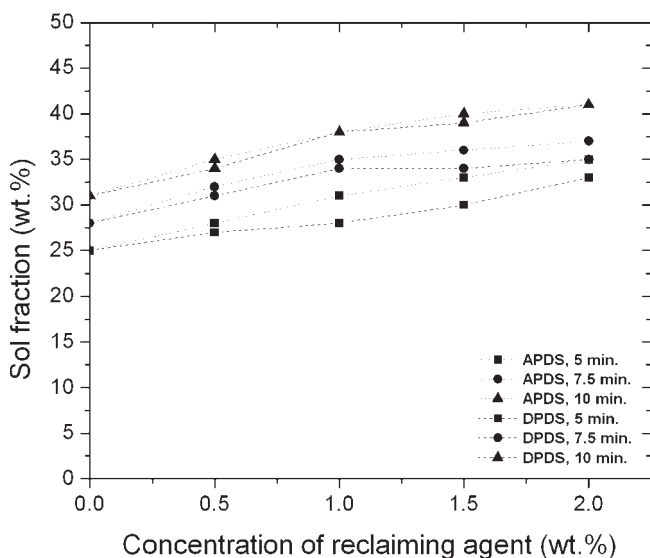


**Figure 13** Sol fraction as a function of concentration of APDS and DPDS at various times for WLR1 at 180°C.

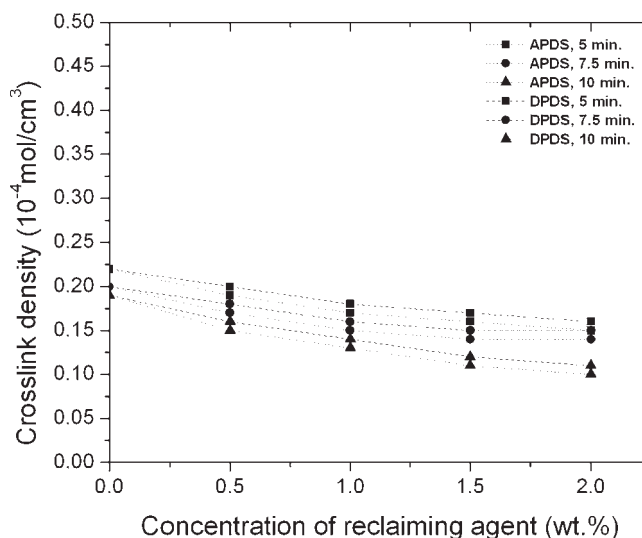


**Figure 14** Crosslink density as a function of concentration of APDS and DPDS at various times for WLR1 at 180°C.

The intrinsic viscosity was determined with a Viscotek H502 viscometer equipped with a refractive index (RI) detector (Waters 410).

The reaction rates and activation energy for the reclamation reaction were calculated using the Mooney viscosity data according to ISO 53,529: The Mooney viscosity, MV, was measured as a function of reclamation time at different temperatures. The reaction constant for a first order reaction was calculated according to the following equations.

$$k_r = \frac{\ln(1 - x_1) - \ln(1 - x_2)}{t_2 - t_1} \quad (2)$$

$$x = \frac{MV_0 - MV(t)}{MV_0 - MV_\infty} \quad (3)$$

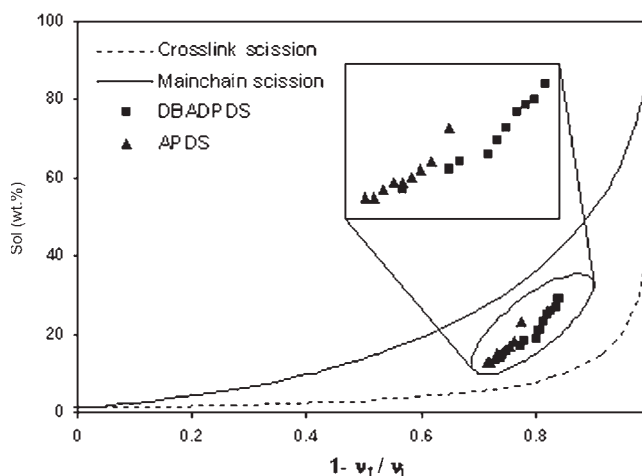


**Figure 15** Fraction of sol of WLR1 against relative decrease in crosslink density at 150°C.

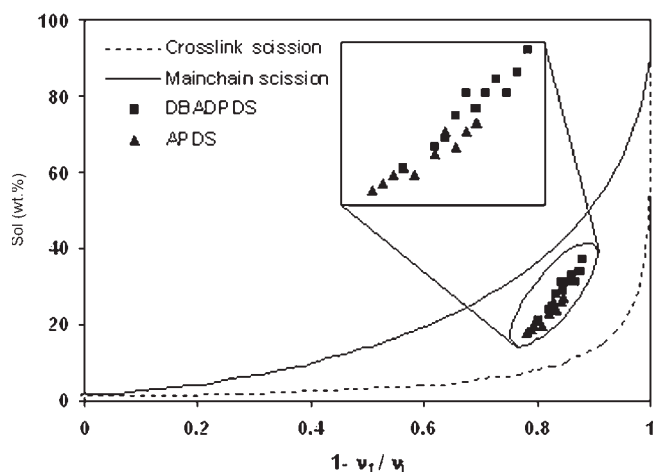


**Figure 16** Fraction of sol of WLR1 against relative decrease in crosslink density at 160°C.

The reaction variable  $x$  was calculated from the Mooney viscosity at time  $t$ ,  $MV(t)$ , the Mooney viscosity of the starting material  $MV_0$  and the Mooney viscosity for an optimally reclaimed sample  $MV_\infty$ . The reaction constant  $k_r$  is given by the slope of the line of the  $\ln(1-x)$  as a function of time, Figure 1.

The activation energy  $E_a$  was calculated from the reaction constants  $k_r$  at different temperatures  $T$  using the Arrhenius equation;

$$\ln k_r \propto -\frac{E_a}{RT} \quad (4)$$

In a graph showing  $\ln k_r$  as a function of the reciprocal temperature, the slope of the line gives the value of the activation energy, as illustrated in Figure 2.

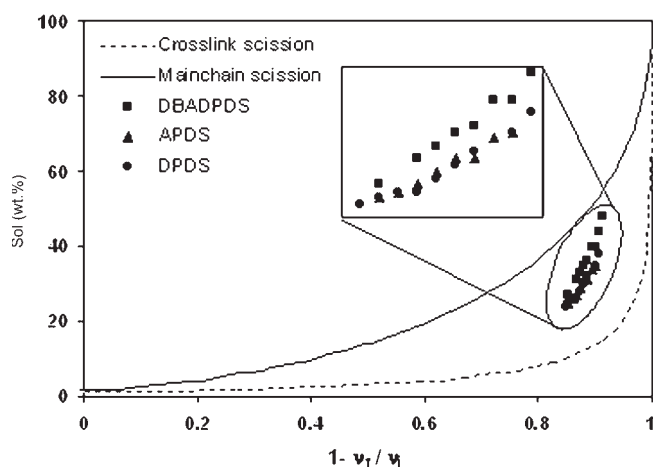


**Figure 17** Fraction of sol of WLR1 against relative decrease in crosslink density at 170°C.

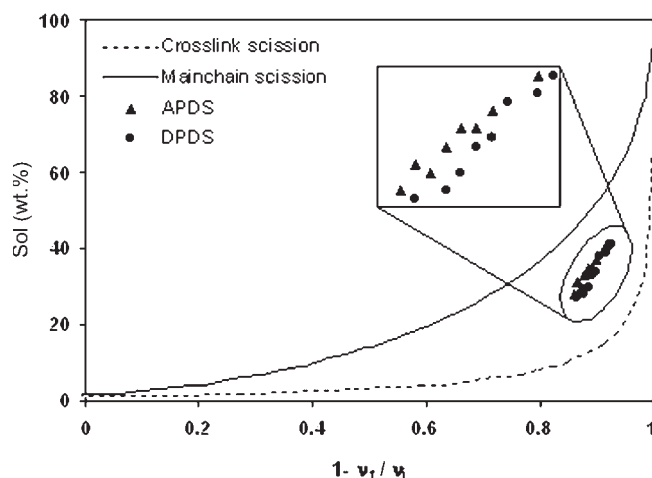


**Figure 18** Fraction of sol of WLR1 against relative decrease in crosslink density at 180°C.

## RESULTS

The effect of DBADPDS, APDS, and DPDS at four different temperatures, viz. 150, 160, 170, and 180°C was studied. At 150 and 160°C, a comparison can only be made between DBADPDS and APDS as DPDS was not reactive at this temperature. At 170°C a comparison is made for all three disulfides. At 180°C, DBADPDS was extremely reactive so that only APDS and DPDS are compared.

### Reclamation of WLR1 with DBADPDS, APDS, and DPDS

Figures 3 and 4 show the Mooney viscosity of WLR1 at various times as a function of the concentration of DBADPDS and APDS at temperatures of 150 and 160°C.

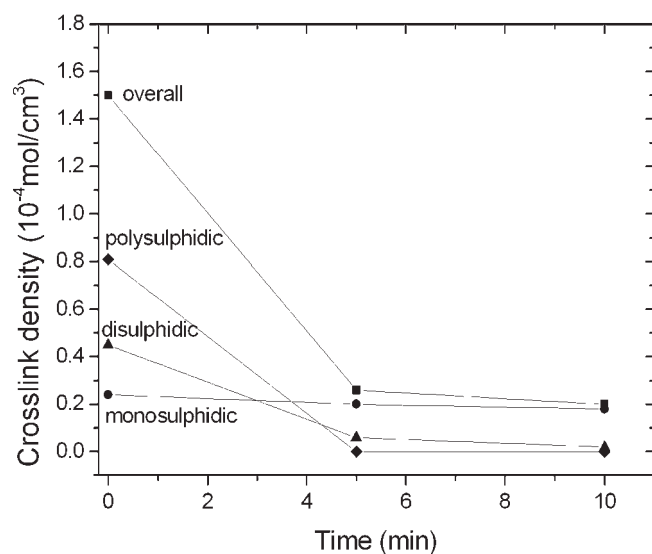


**Figure 19** Crosslink distribution of WLR1 reclaimed with DBADPDS as a function of reclaiming times at 160°C.

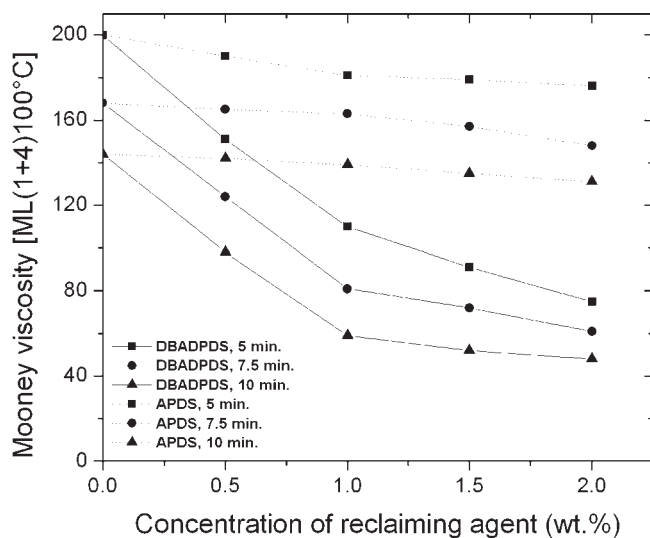


**Figure 20** Mooney viscosity as a function of concentration of DBADPDS and APDS at various times for WLR2 at 150°C.

**DBADPDS:** The Mooney viscosity decreases for DBADPDS with increasing concentration of reclaiming agent and reclamation time at both temperatures. There is a strong decrease in Mooney viscosity up to a concentration of 1 wt %; at higher concentrations the rate of viscosity decrease slows down. The decrease in viscosity shows the same trends for all temperature/time profiles. The viscosity level is in general lower than in the case of APDS as reclaiming agent.

**APDS:** The increase in concentration of APDS has little effect on the Mooney viscosity of WLR1 after reclamation at 150 and 160°C. With increasing recla-

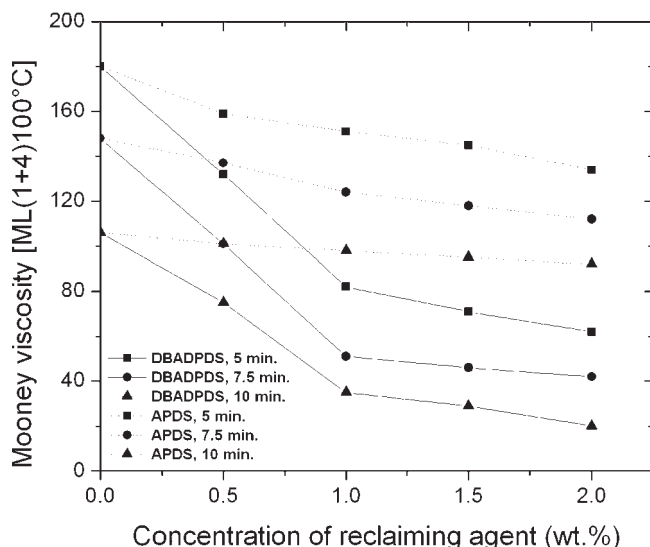


**Figure 21** Mooney viscosity as a function of concentration of DBADPDS and APDS at various times for WLR2 at 160°C.

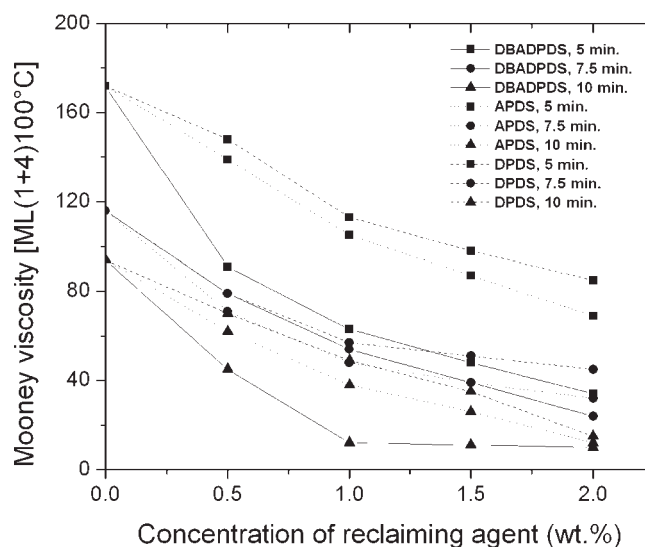


**Figure 22** Mooney viscosity as a function of concentration of DBADPDS, APDS, and DPDS at various times for WLR2 at 170°C.

mation time the Mooney viscosity of WLR1 decreases, probably because of mechanical breakdown of the vulcanizate rather than to the chemical influence of APDS. The Mooney viscosity decreases less at 150°C compared to 160°C: At a higher temperature the decrease in viscosity due to the thermal effect is stronger.<sup>17</sup>

The Mooney viscosity of WLR1 at various times as a function of the concentration of DBADPDS, APDS, and DPDS at 170°C is depicted in Figure 5. With DBADPDS as reclaiming agent the viscosity decreases much faster than with APDS and DPDS, but the decrease levels off for higher concentrations of

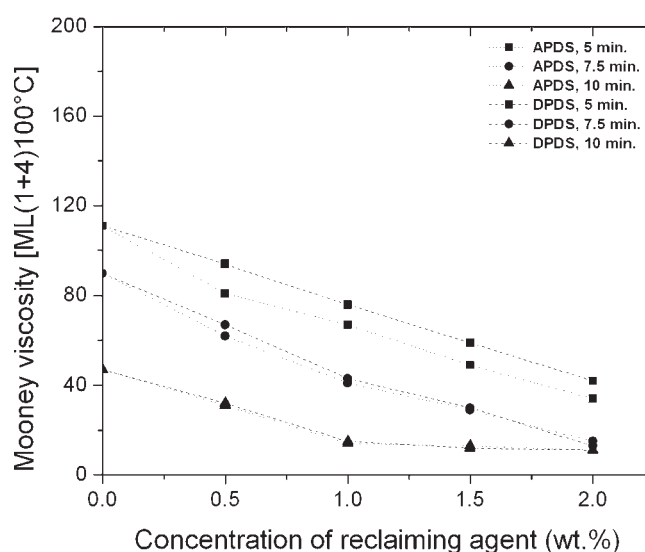


**Figure 23** Mooney viscosity as a function of concentration of APDS and DPDS at various times for WLR2 at 180°C.



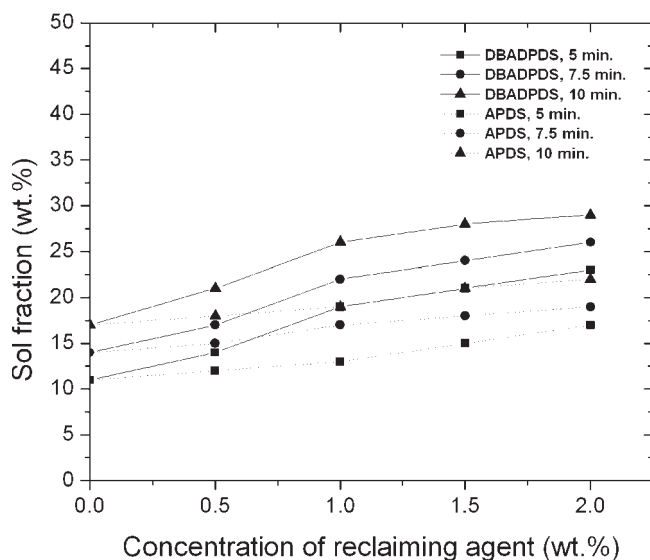


**Figure 24** Sol fraction as a function of concentration of DBADPDS and APDS at various times for WLR2 at 150°C.

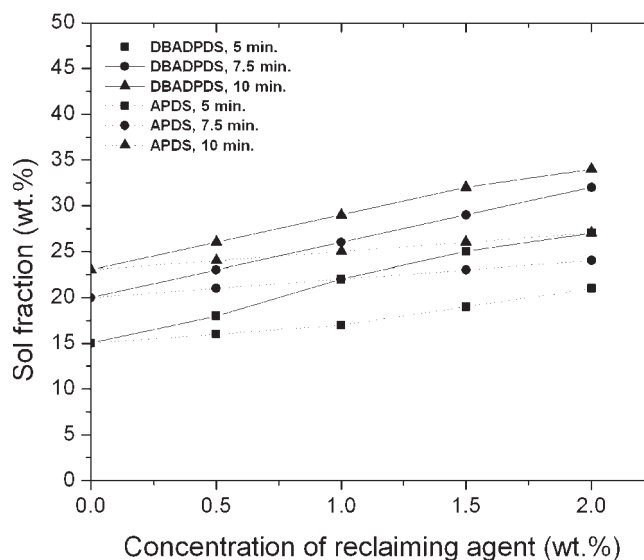


**Figure 26** Sol fraction as a function of concentration of DBADPDS and APDS at various times for WLR2 at 160°C.

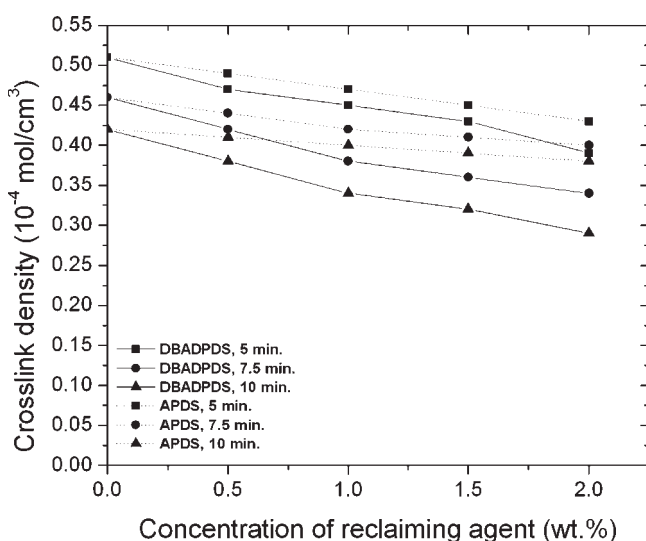
DBADPDS. DPDS has the smallest effect on the viscosity of the vulcanizate.

Figure 6 gives the Mooney viscosity of WLR1 at various times against the concentration of APDS and DPDS at 180°C. Both reclaiming agents cause a linear decrease of the viscosity of WLR1 with increasing concentration of the reclaiming agent at this temperature. An increase in reclamation time also results in a decrease of the viscosity. Only small differences in the viscosity values are found for WLR1 treated with APDS compared to DPDS at 180°C.

Figures 7–10 show the sol fraction and crosslink density for WLR1 at various times as a function of

the concentration of DBADPDS and APDS at temperatures of 150 and 160°C, respectively. The sol fraction increases and correspondingly the crosslink density decreases for DBADPDS. At 160°C a stronger increase in sol fraction and decrease in crosslink density is found because of the increase in reactivity of DBADPDS with increasing temperature. The increase in concentration of APDS has less influence on the sol fraction and crosslink density of the vulcanizate at these temperatures compared to DBADPDS as reclaiming agent.

The sol fraction and crosslink density of WLR1 at various times as a function of concentration of the



**Figure 25** Crosslink density as a function of concentration of DBADPDS and APDS at various times for WLR2 at 150°C.

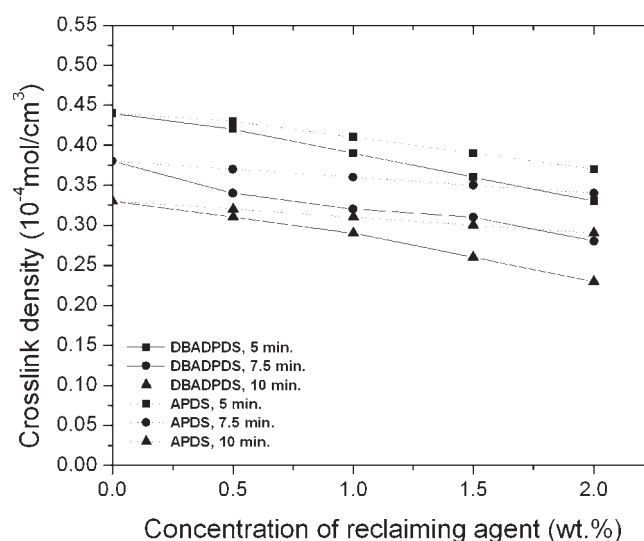


**Figure 27** Crosslink density as a function of concentration of DBADPDS and APDS at various times for WLR2 at 160°C.

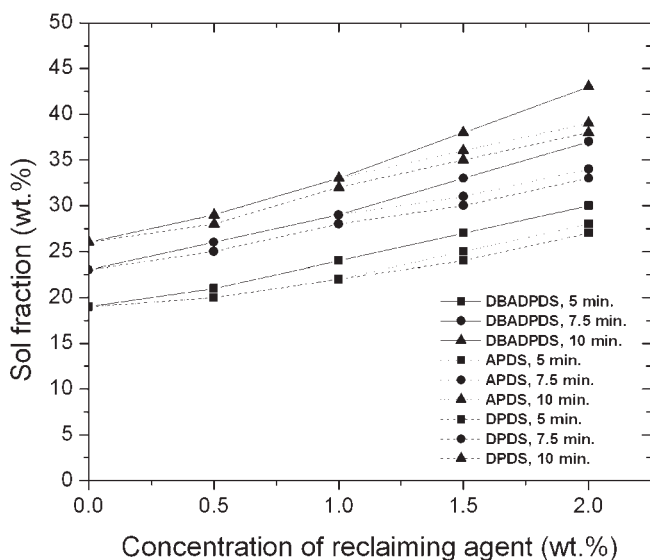


**Figure 28** Sol fraction as a function of concentration of DBADPDS, APDS, and DPDS at various times for WLR2 at 170°C.

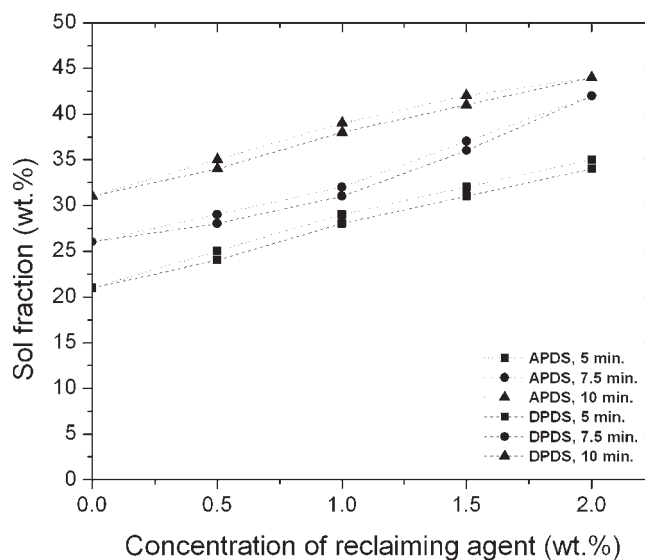


**Figure 30** Sol fraction as a function of concentration of APDS and DPDS at various times for WLR2 at 180°C.

reclaiming agents at 170°C is given in Figures 11 and 12. Again, DBADPDS is more efficient than the other two reclaiming agents, and a significant increase in sol fraction and decrease in crosslink density is measured at this temperature.

Figures 13 and 14 depict the sol fraction and crosslink density of WLR1 as a function of the concentration of the reclaiming agents at 180°C. As expected, the sol fraction increases and crosslink density decreases with increase in concentration of both reclaiming agents, but at high degrees of reclamation the sol fraction and crosslink density level off. Only

small differences are seen in the values of both properties for the two reclaiming agents: their reactivity at this temperature is quite similar, as already seen in Figures 11 and 12 for lower temperature.

It is important to know whether the reaction with DPDS is mainly based on main-chain scission or crosslink scission. Horikx has developed the theoretical relationship between the soluble fraction after degradation of a network and the relative decrease in crosslink density as a result of either main-chain scission or crosslink scission.<sup>18</sup> When, only main-chain scission takes place, the relative decrease in crosslink density is given by the following equation:

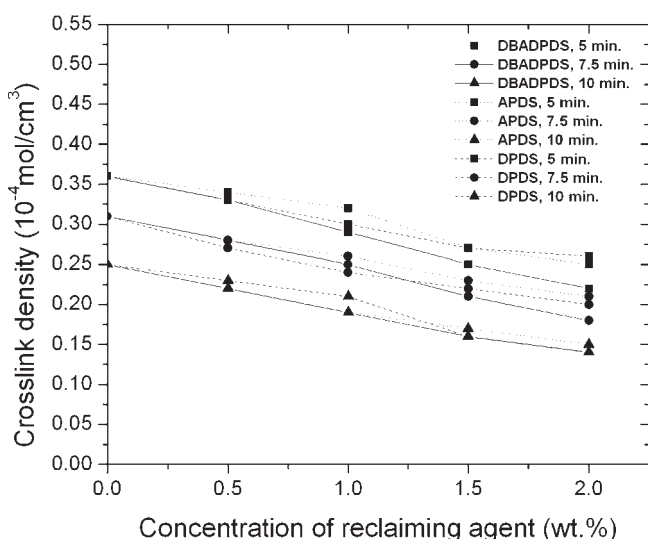


**Figure 29** Crosslink density as a function of concentration of DBADPDS, APDS, and DPDS at various times for WLR2 at 170°C.

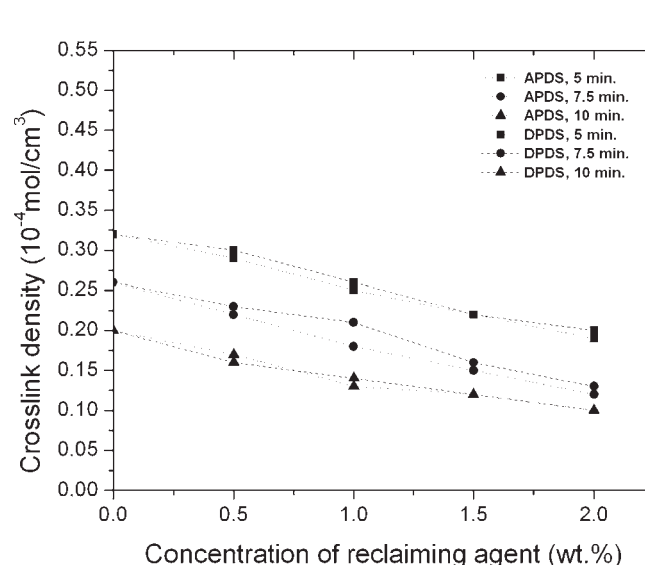


**Figure 31** Crosslink density as a function of concentration of APDS and DPDS at various times for WLR2 at 180°C.

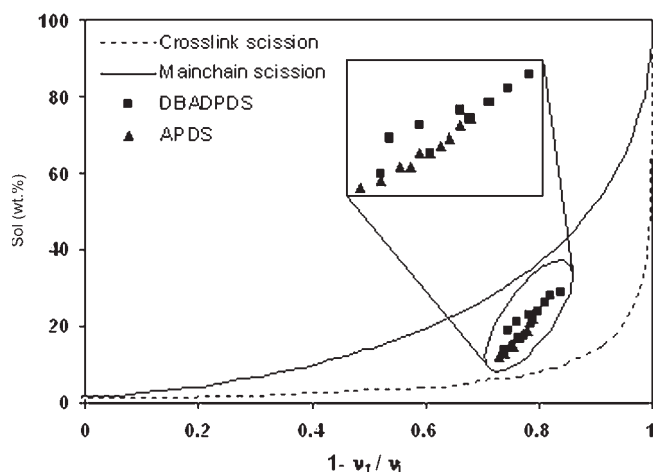


**Figure 32** Fraction of sol of WLR2 against relative decrease in crosslink density at 150°C.

$$1 - \left(\frac{v_f}{v_i}\right) = 1 - \left[\frac{(1 - s_f^{1/2})^2}{(1 - s_i^{1/2})^2}\right] \quad (5)$$

where  $s_i$  is the soluble fraction of the virgin untreated vulcanizate,  $s_f$  the soluble fraction of reclaimed vulcanizate,  $v_i$  is the crosslink density of the untreated vulcanizate, and  $v_f$  the crosslink density of the reclaimed vulcanizate.

For crosslink scission the soluble fraction is related to the relative decrease in crosslink density by equation:

$$1 - \left(\frac{v_f}{v_i}\right) = 1 - \left[\frac{\gamma_f(1 - s_f^{1/2})^2}{\gamma_i(1 - s_i^{1/2})^2}\right] \quad (6)$$

where the parameters  $\gamma_i$  and  $\gamma_f$  are the average number of crosslinked units per chain before and after

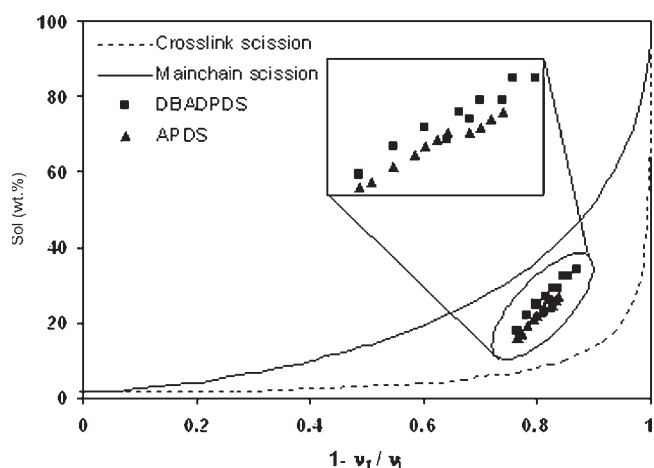


**Figure 33** Fraction of sol of WLR2 against relative decrease in crosslink density at 160°C.

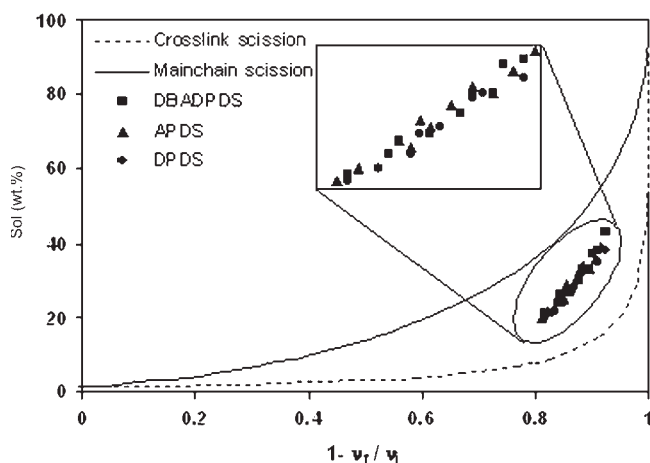


**Figure 34** Fraction of sol of WLR2 against relative decrease in crosslink density at 170°C.

reclamation, respectively. These numbers are calculated from the sol fraction.

The sol fraction of WLR1 as a function of the relative decrease in crosslink density for DBADPDS and APDS at 150 and 160°C is depicted in Figures 15 and 16. The curves in both figures show the two extreme cases: One corresponds to the situation where only main-chains are broken (solid curve), and the other corresponds to breaking of crosslinks (dotted curve). For crosslink scission almost no sol is formed until most of the crosslinks are broken, only then the long chains can be removed. In the case of main-chain scission, sol is produced in an early stage because the random scission of the polymer network results in loose chain fragments, which can easily be removed.<sup>19,20</sup> In Figures 15 and 16 the experimental data for breakdown of WLR1 with DBADPDS and APDS lie in-between the main-chain scission curve and crosslink scission curve. The sol fraction values

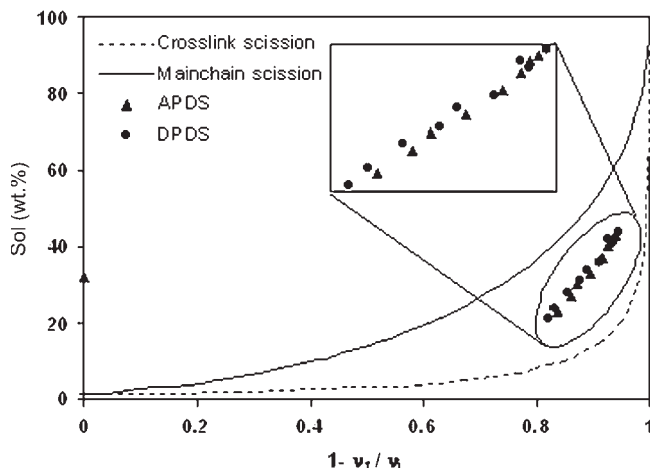


**Figure 35** Fraction of sol of WLR2 against relative decrease in crosslink density at 180°C.

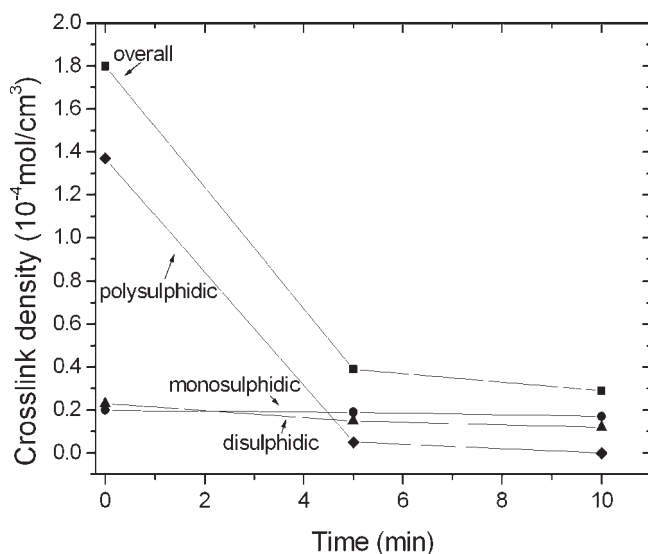


**Figure 36** Crosslink distribution of WLR2 reclaimed with DBADPDS as a function of reclaiming times at 160°C.

of the experiments are significantly lower than the values predicted for main-chain scission. This indicates that the reclamation occurred mainly through crosslink scission.

The sol fraction of WLR1 as a function of the relative decrease in crosslink density at 170 and 180°C are depicted in Figures 17 and 18. Both reclaiming agents break the vulcanizate mainly by crosslink scission as aforementioned. In Figure 17, the experimental data points for WLR1 reclaimed with DBADPDS are very close to the main-chain rupture curve (solid curve) showing a lot of main-chain scission occurring at this stage. On analyzing the experimental condition for this particular case it becomes clear that these data belong to the extreme conditions

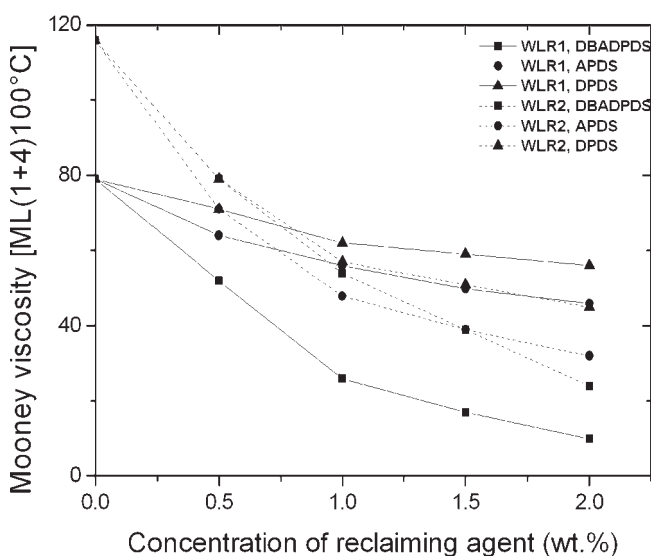


**Figure 37** Mooney viscosity of WLR1 and WLR2 as a function of concentration of the reclaiming agent at 170°C.

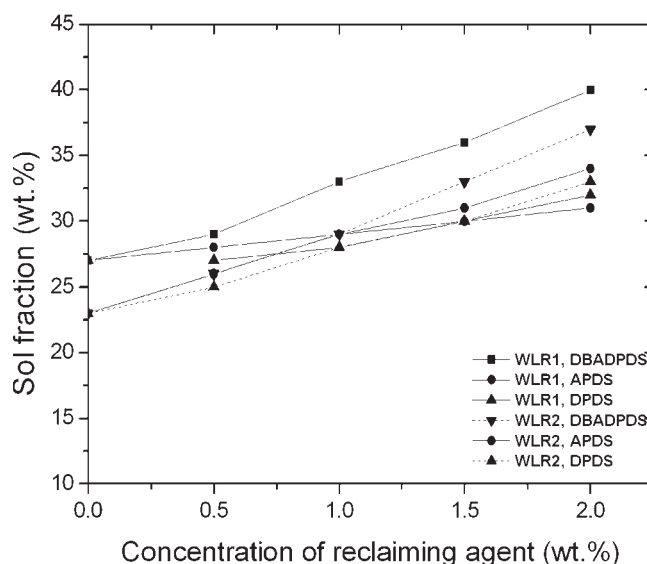


**Figure 38** Sol fraction of WLR1 and WLR2 as a function of concentration of the reclaiming agent at 170°C.

of 170°C, 2 wt % of reclaiming agent and 10 min of reclamation time: These conditions are apparently critical for the feed-stock and resulted in a significant breakage of main-chains.

GPC measurements of the sol fraction of DBADPDS reclaimed samples showed that the number-average molecular weight ( $M_n$ ) of WLR1 decreased from  $2.6 \times 10^5$  g/mol to  $4.7 \times 10^4$  g/mol at 160°C and 1 wt % of reclaiming agent. Increasing the concentration of DBADPDS from 1 to 2 wt % did not result in a further decrease of the molecular weight of the polymer in the sol fraction.

The crosslink densities of WLR1 reclaimed with DBADPDS as a function of the reclaiming time at 160°C are presented in Figure 19. The concentration

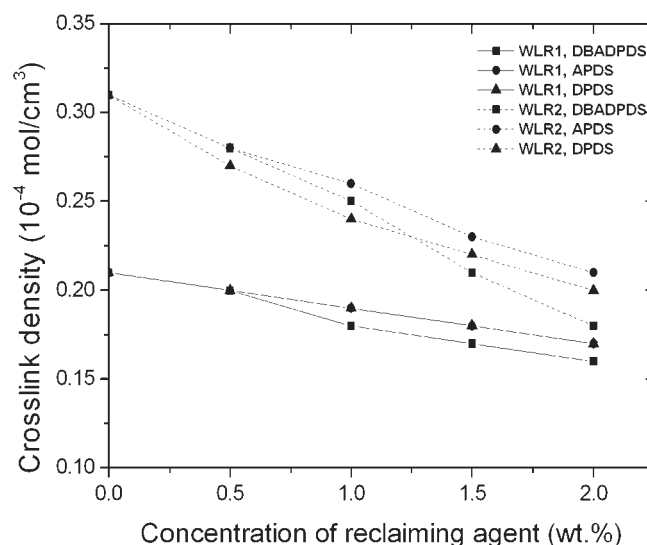


**Figure 39** Crosslink density of WLR1 and WLR2 as a function of concentration of the reclaiming agent at 170°C.

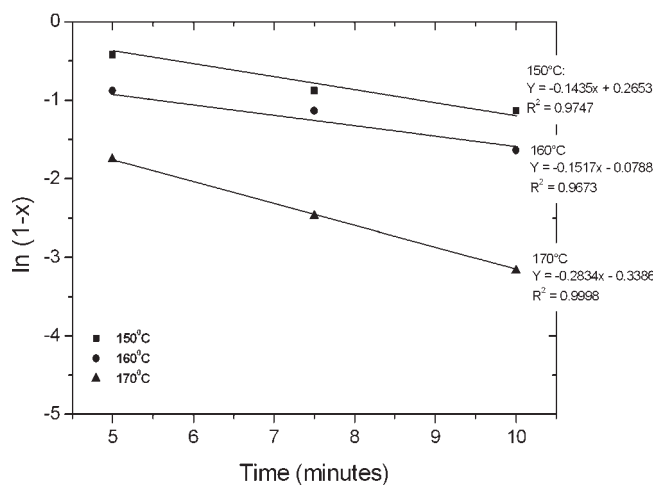


**Figure 40** Determination of rate constant for WLR1 with DBADPDS at different temperatures.

of crosslinks as well as the fraction of poly- and disulfidic crosslinks decrease, whereas the concentration of monosulfidic crosslinks remains constant with reclamation time. The polysulfidic and disulfidic crosslinks diminish, but the overall crosslink density decreases to the level of the monosulfidic crosslinks: after reclamation the remaining crosslinks present in WLR1 are mainly monosulfidic. This is caused by the higher bonding energy of monosulfidic crosslinks compared with the bonding energies of poly- or disulfidic crosslinks.<sup>21,22</sup>

#### Reclamation of WLR2 with DBADPDS, APDS, and DPDS

The Mooney viscosity of WLR2 as a function of the concentration of DBADPDS and APDS at tempera-

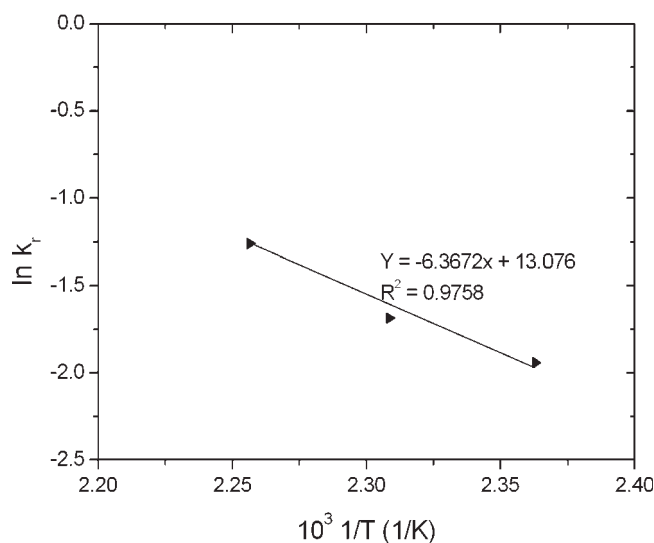


**Figure 41** Determination of activation energy of reclamation for WLR1 with DBADPDS at different temperatures.

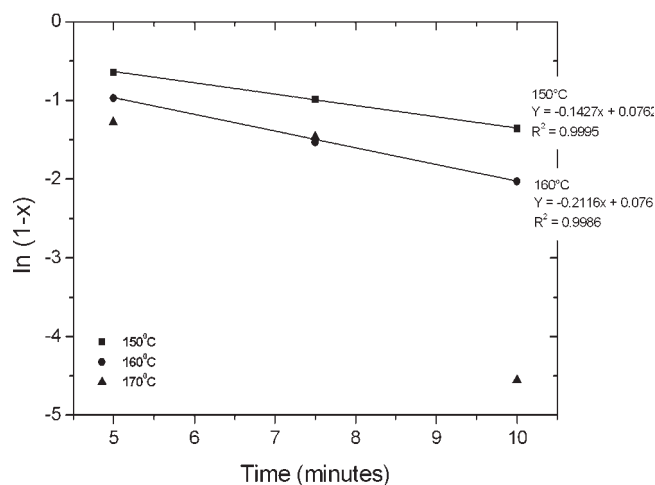


**Figure 42** Determination of rate constant for WLR2 with DBADPDS at different temperatures.

tures of 150 and 160°C at various times is presented in Figures 20 and 21. A significant decrease in viscosity for DBADPDS as reclaiming agent is observed at both temperatures and the decrease in viscosity is much faster for concentrations up to 1 wt %; at higher concentrations it levels off. The decrease in Mooney viscosity observed with APDS at these temperatures is less pronounced.

Figure 22 shows the Mooney viscosity of WLR2 at various times as a function of DBADPDS, APDS, and DPDS at 170°C. The viscosity decreases with increasing concentration for all reclaiming agents and for longer reclamation times. DBADPDS is the most effective reclaiming agent by far at medium concentrations. At short reclaiming periods the viscosity is drastically reduced by DBADPDS. DPDS

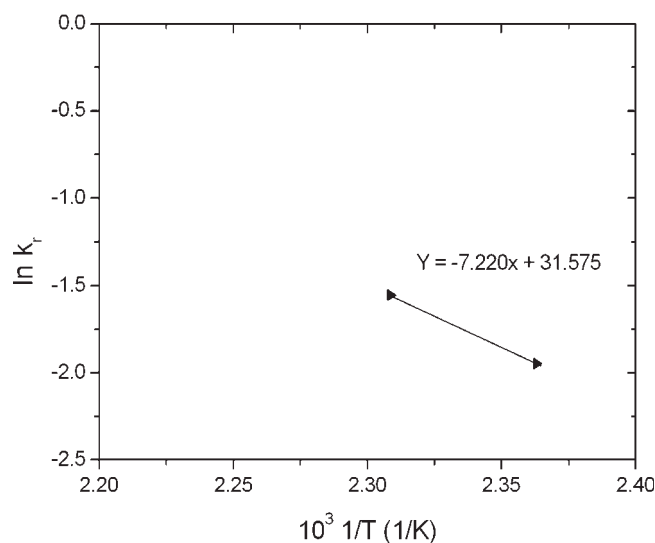


**Figure 43** Determination of activation energy of reclamation for WLR2 with DBADPDS at different temperatures.

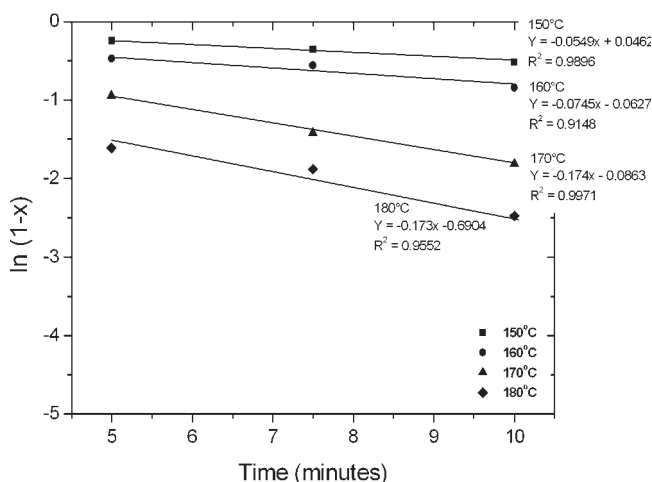


**Figure 44** Determination of rate constant for WLR1 with APDS at different temperatures.

and APDS also reduce the viscosity but they are less effective compared to DBADPDS. At longer reclamation times and at high concentrations of reclaiming agent, the viscosity values are comparable for all reclaiming agents.

The Mooney viscosity of WLR2 as a function of the concentration of APDS and DPDS at 180°C and at various times is given in Figure 23. The reactivity is similar for both reclaiming agents. For short reclamation times APDS is slightly more reactive than DPDS.

The sol fraction and crosslink density of WLR2 as a function of the concentration of DBADPDS and APDS at 150 and 160°C at various times is shown in Figures 24–27. The sol fraction and crosslink density of the DBADPDS reclaimed samples show a stronger change than those of APDS reclaimed samples at

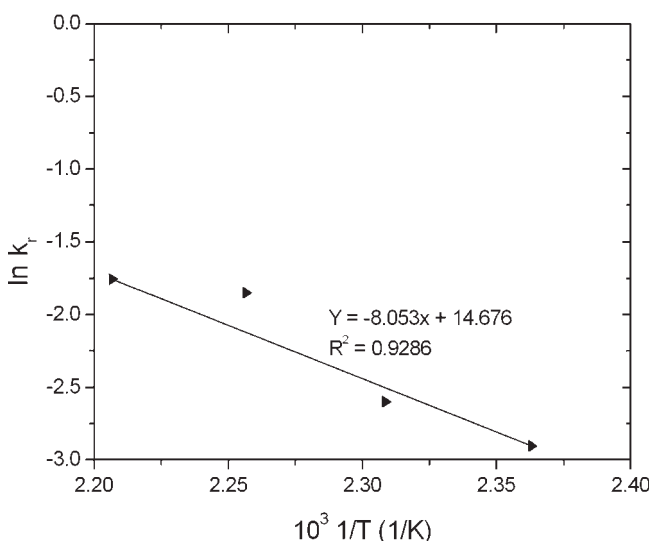


**Figure 45** Determination of activation energy of reclamation for WLR1 with APDS at different temperatures.

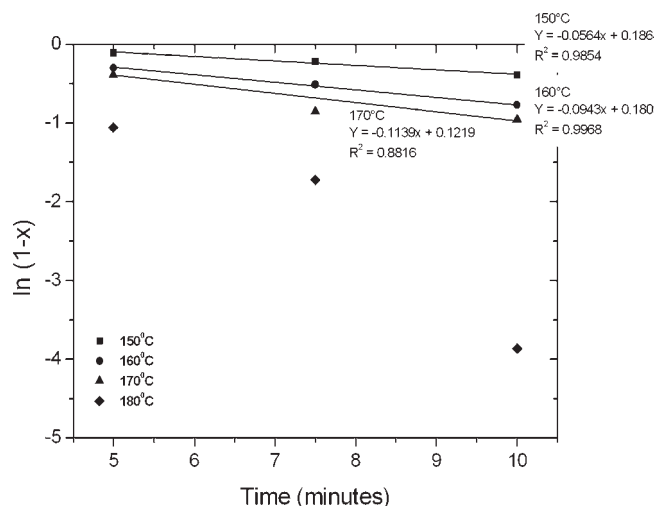


**Figure 46** Determination of rate constant for WLR2 with APDS at different temperatures.

both temperatures. DBADPDS is breaking down the three dimensional structure of the vulcanized material more easily, through both crosslink scission and main-chain rupture.

Figures 28 and 29 present the sol fraction and crosslink density of WLR2 against the concentration of the three reclaiming agents at 170°C and Figures 30 and 31 show the data at 180°C. The sol fraction increases and the crosslink density decreases linearly with increasing concentration of all reclaiming agents. The three reclaiming agents are effective in reclaiming WLR2, and DBADPDS is slightly more effective than the other two reclaiming agents at 170°C. APDS and DPDS work better for WLR2 at 170 and 180°C compared to their performance with

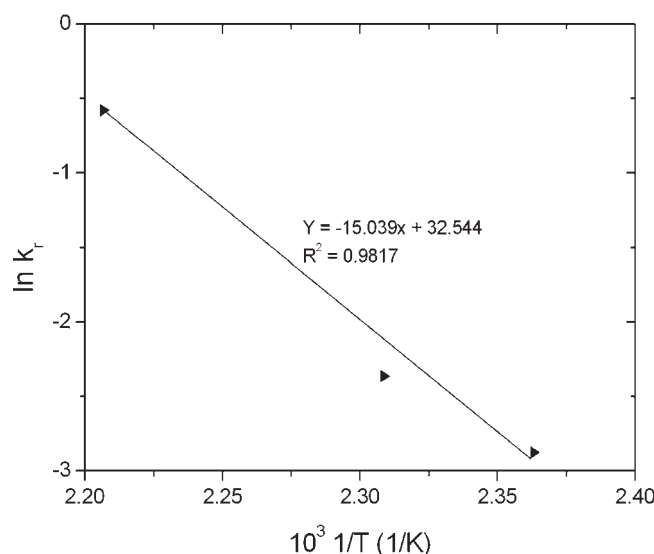


**Figure 47** Determination of activation energy of reclamation for WLR2 with APDS at different temperatures.

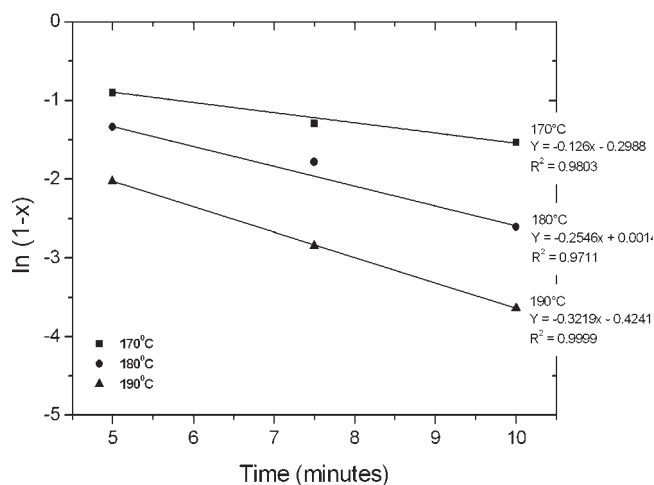


**Figure 48** Determination of rate constant for WLR1 with DPDS at different temperatures.

WLR1 in breaking down the vulcanizate; compare Figures 11–14.

Figures 32 and 33 show the sol fraction of WLR2 as a function of the relative decrease in crosslink density for DBADPDS and APDS at 150 and 160°C. As explained for Figures 15 and 16 the reclamation is mainly occurring through crosslink scission rather than by main chain scission, because the experimental data points are far from the main-chain scission curve (solid curve). The same result is observed in Figures 34 and 35, which depicts the sol fraction of WLR2 against the relative decrease in crosslink density for DBADPDS, APDS and DPDS at 170 and 180°C, respectively.

In Figures 32 and 33 the experimental points with DBADPDS lie slightly closer to main-chain scission curve compared to APDS; however, in other cases, Figures 34 and 35 no significant difference is observed

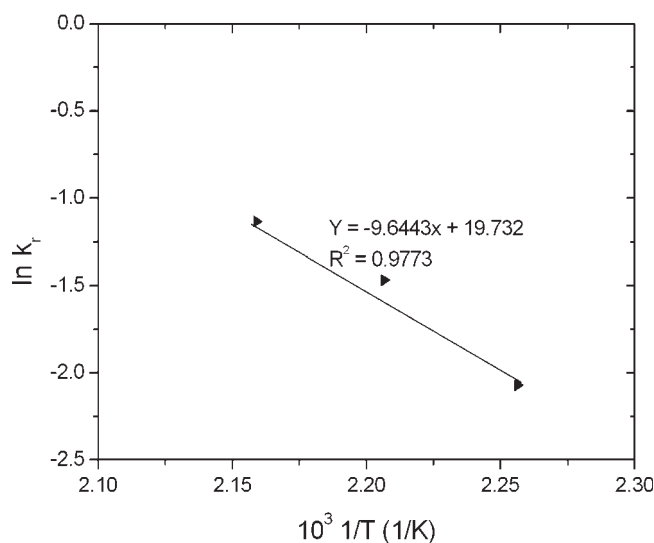


**Figure 49** Determination of activation energy of reclamation for WLR1 with DPDS at different temperatures.

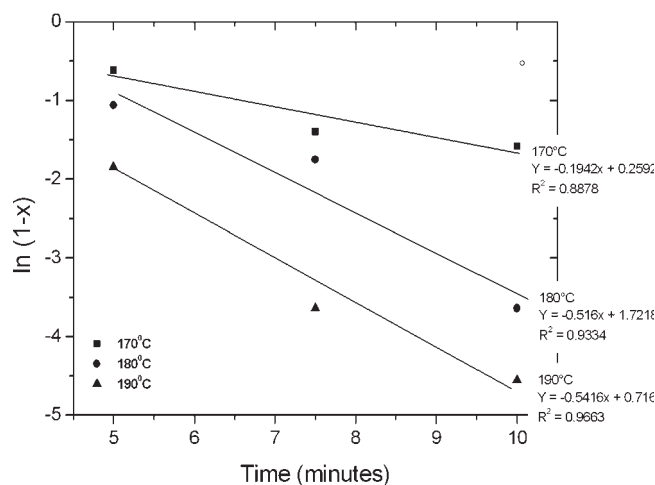


**Figure 50** Determination of rate constant for WLR2 with DPDS at different temperatures.

between the behavior of DBADPDS, APDS, and DPDS. This observation is in contradiction to WLR1 (Figs. 15–18), where DBADPDS is closer to main-chain scission in almost all cases compared to APDS.

The crosslink densities of WLR2 reclaimed with DBADPDS as a function of reclaiming time at 160°C is depicted in Figure 36. The overall crosslink density and the concentration of poly- and disulfidic crosslinks decrease, whereas the monosulfidic crosslink density remains constant with reclaiming time. This shows that DBADPDS is not able to break the monosulfides present in the rubber network, as seen for WLR1 in Figure 19.

#### Comparison of reclamation of WLR1 and WLR2 with DBADPDS, APDS, and DPDS

The change in Mooney viscosity, sol fraction and crosslink density of WLR1 and WLR2 with increasing concentration of DBADPDS, APDS, and DPDS at 170°C and 7.5 min is presented in Figures 37–39. The Mooney viscosity and crosslink density of WLR1 and WLR2 decrease and consequently the sol fraction increases with increase in the concentration of the reclaiming agents. The initial viscosity and crosslink density of WLR1, when the concentration of the reclaiming agent is 0 wt %, is lower than that of

**TABLE IV**  
Kinetic Data for the Reclamation of WLR1 and WLR2 with DBADPDS

Rate of reclamation with DBADPDS		
Temperature (°C)	WLR1 $k_r$ (min <sup>-1</sup> )	WLR2 $k_r$ (min <sup>-1</sup> )
150	0.1435	0.1427
160	0.1517	0.2116
170	0.2834	—
Activation energy, $E_a$ (kJ/mol)	53	60

**TABLE V**  
Kinetic Data for the Reclamation of WLR1 and WLR2 with APDS

Rate of reclamation with APDS		
Temperature (°C)	WLR1 $k_r$ (min <sup>-1</sup> )	WLR2 $k_r$ (min <sup>-1</sup> )
150	0.0549	0.0564
160	0.0745	0.0943
170	0.173	0.1139
180	0.174	–
Activation energy, $E_a$ (kJ/mol)	67	125

WLR2; but as the concentration of the reclaiming agents increases, WLR2 shows a more substantial reduction in viscosity and crosslink density compared to WLR1. The sol fraction values of WLR1 and WLR2 follow a similar trend. DBADPS shows a different behavior: The initial values of WLR1 follow the same pattern as the other reclaiming agents but at no stage of the reaction the viscosity or crosslink density is lower for WLR2 compared to WLR1. A possible explanation is a higher reactivity of DBADPS at 170°C, breaking more main-chains under these extreme conditions. This is also visible in Figure 17, where the position of the points for DBADPS indeed points to more main-chain scission relative to crosslink scission of WLR1 relative to the other two agents.

#### Kinetics of the reclamation reaction with DBADPDS, APDS, and DPDS

Figures 40 through 50 and Tables IV–VI show the results of the kinetic study of different series of reclamation reactions carried out with different reclaiming agents and feed stocks. The temperature range of the reactions was from 150 to 190°C and the reclamation times were 5, 7.5, and 10 min. The lowest achievable values of the Mooney viscosity for each reclaiming agent, necessary for the calculation of the reaction rate constants was measured for WLR1 and WLR2 after reclamation at 170°C and 10 min with DBADPDS, 180°C and 10 min with APDS, and 190°C and 7.5 min with DPDS. The initial Mooney viscosity was taken as the viscosity attainable with the mild reclamation conditions on the feedstocks and was measured as 200 MU.

Figures 40–43 show graphical representations of the calculation of rate constant and activation energy for the reclamation of WLR1 and WLR2 at temperatures of 150, 160, and 170°C with DBADPDS.

In Figures 42 and 43, the data points for the reclamation of WLR2 with DBADPDS at 170°C do not show a linear correlation with reclaiming time. This shows that this material reacts according to a different reaction mechanism at this temperature and therefore a different order for the reaction has to be

assumed. The highest feasible experimental temperature with DBADPDS is 170°C, and this probably causes several side reactions to occur with WLR2.

Table IV shows the of rate constants at the different temperatures and activation energies for WLR1 and WLR2. At 150°C, WLR1 and WLR2 have comparable rate constants, but the rate constant of WLR2 is higher than the reaction rate of WLR1 at 160°C. At 170°C there is a significant increase in the rate constant for WLR1. The activation energies of both feedstocks were calculated for the temperature range given in Table IV: the activation energies are in the same order of magnitude, as can be seen in Table IV and from the slope of the graph in Figures 41 and 43.

Figures 44–47 show a graphical representation of the calculation of the rate constants and activation energies for the reclamation of WLR1 and WLR2 at temperatures of 150, 160, 170, and 180°C with APDS. Table V gives the rate constants of the comparative investigation of the reclamation of WLR1 and WLR2 with APDS at temperatures of 150, 160, 170, and 180°C. At 150 and 160°C the rate constants do not vary significantly depending on the feedstock, the reaction rates for the reclamation with APDS are significantly lower compared to DBADPDS as reclaiming agent. Between 160 and 170°C there is a large increase in the rate constant for WLR1. Surprisingly, at 180°C the rate constant of WLR1 differs not from the value at 170°C. The activation energies of both reclaiming materials show that WLR2 has a higher temperature dependence than WLR1, represented by a higher activation energy and the activation energy for the reclamation of WLR2 is higher for APDS compared to DBADPDS as reclaiming agent.

Figures 48–50 is the graphical representation of the calculation of the rate constants and activation energies for the reclamation of WLR1 and WLR2 at temperatures of 170, 180, and 190°C with DPDS. Table VI gives the reaction rate constants and activation energy for DPDS reclaimed samples. An increase of the reaction rate for WLR1 is seen with increase in temperature. A large increase in the rate constant for WLR2 is found when the temperature is increased from 170 to 180°C, with almost no further change of the rate constant when the temperature is

**TABLE VI**  
Kinetic Data for the Reclamation of WLR1 and WLR2 with DPDS

Rate of reclamation with DPDS		
Temperature (°C)	WLR1 $k_r$ (min <sup>-1</sup> )	WLR2 $k_r$ (min <sup>-1</sup> )
170	0.126	0.1942
180	0.2546	0.516
190	0.3219	0.5416
Activation energy, $E_a$ (kJ/mol)	73	–



TABLE VII  
Distribution of Different Types of Sulfur Crosslinks in NR Vulcanizates Before Reclamation

Feed stock	Overall crosslink density, $v_c$ ( $10^{-4}$ mol/cm <sup>3</sup> )	Monosulphidic ( $10^{-4}$ mol/cm <sup>3</sup> )	Disulphidic ( $10^{-4}$ mol/cm <sup>3</sup> )	Polysulphidic ( $10^{-4}$ mol/cm <sup>3</sup> )
WLR1	1.5	0.24 (16%)	0.45 (30%)	0.81 (54%)
WLR2	1.8	0.20 (11%)	0.23 (13%)	1.37 (76%)

increased to 190°C. The activation energy of the reclamation of WLR1 with DPDS is higher than the activation energy of the reaction with DBADPDS: the reaction with DPDS is more temperature-dependent. The activation energy of WLR2 could not be calculated because the correlation between  $\ln k_r$  and  $1/T$  is not linear, probably because of a change in the reaction mechanism within the temperature interval.

### DISCUSSION

The crosslink density and the crosslink types of WLR1 and WLR2 before reclamation determined by swelling measurements in combination with reaction of thiol-amine reagents for the two base materials are given in Table VII. These data are important, because the crosslink scission during reclamation in sulfur vulcanizates depends on the type and amount of sulfidic linkages. It is well known that the bond energy of the monosulfidic crosslinks is higher than that of poly- or disulfidic crosslinks,<sup>21,22</sup> which means that a sulfur vulcanizate with a lower percentage of monosulfidic crosslinks will reclaim easier.

The results presented in the above figures comprehensively point to the fact that DBADPDS reclaims a NR vulcanizate more efficiently than the other two reclaiming agents used in this investigation. The reactivity of reclaiming agents used shows the following trend:



All three reclaiming agents can in principle be represented as derivatives of one basic structure, as represented by Figure 51, where in the case of DPDS the  $-\text{NH}-\text{R}$  substituents are absent, in the case of APDS the  $-\text{R}$  group equals hydrogen, and in the

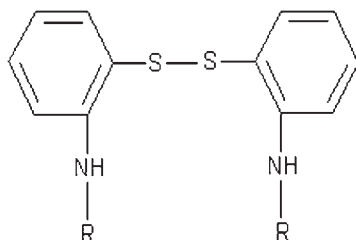
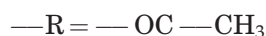


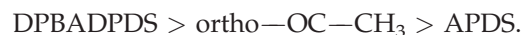
Figure 51 General representation of reclaiming agents.

case of DBADPDS, the  $-\text{R}$  group represents  $\text{C}_6\text{H}_5\text{CO}-$ .

In an elementary study dating back to 1952, Imoto and Kiriya<sup>23</sup> have investigated the reactivity towards NR of several variants on the general structure in Figure 51, wherein they made the following variations, with the substituents in the ortho-, resp. in the *para*-position relative to the disulfide-bridge:



Applying dilute amounts of these agents in a 0.85 wt % solution of Smoked Sheet NR (SSNR) in toluene, they measured the decrease in viscosity of the solution in an Ostwald viscosimeter against time, at 40, 50, and 60°C. It was observed, that the agents with the substituents in the *ortho*-position were generally more active than those with the substituents in the *para*-position. Next, the order of reactivity found was:



This agrees well with the observations presented in this thesis.

Imoto and Kiriya further managed to calculate as sort of activation energy for the reaction of the reclaiming agents with the NR-solution using the equation

$$\frac{1}{z} = ke^{-E/RT} \quad (7)$$

where  $z$  was taken as the time necessary to achieve a (somewhat arbitrarily chosen) viscosity, which is proportional to the reaction velocity,  $k$  is an arbitrary constant,  $E$  is the activation energy for the viscosity decrease (in Calories),  $R$  the gas constant, and  $T$  the absolute temperature.

The activation energies for the decrease of the viscosity are given in Table VIII, with the different groups to replace  $-\text{R}$  in Figure 51. The authors did not give the activation energies on a molar basis but only in absolute energy values. So, apart from the ranking of the values, a full comparison with the data obtained in the present work cannot be made.

TABLE VIII  
Activation Energies

-R group	Activation energy: Imoto and Kiriyaama.[23], SSNR (Calories)	Activation energy: present work	
		WLR1 (kJ/mol)	WLR2 (kJ/mol)
DPDS	–	73	–
ortho: H– (APDS)	7000	67	125
para: H–	9400	–	–
ortho: CH <sub>3</sub> CO–	6300	–	–
ortho: C <sub>6</sub> H <sub>5</sub> CO– (DBADPDS)	5800	53	60

Clearly, the ranking of the activation energies confirm that substituents attached to the phenyl group lead to a decreasing efficiency as R- changes from *ortho*-C<sub>6</sub>H<sub>5</sub>CO– (= DBADPDS), over *ortho*-CH<sub>3</sub>CO– to *ortho*-H– (= APDS).<sup>24,25</sup>

The activation energies for WLR1 and WLR2 reclaimed with DPDS, APDS and DBADPDS, as taken from Tables IV–VI are also inserted in Table VIII. A full comparison with the results of Imoto et al. cannot be made, because they investigated partly different compounds in a completely different environment, for a significantly different temperature range of 40–60°C, versus the present work: 150–180°C, and made use of another sort of Arrhenius-eq. (7), relative to the eq. (4) in the present work. Still there is a reasonably good agreement between the two series of experiments, at least confirming the order of the reactivities found in the present work.

The viscosity decrease of the NR-solutions was claimed by Imoto et al. to be the result of main chain scission. Obviously, because in the solution there was no sulfur-based crosslink network present. The high reactivity of the agent with the C<sub>6</sub>H<sub>5</sub>CO-group in the *o*-position was then quoted to be the result of easy breakage of the S-S bond, resulting in a higher level of sulfidic radicals than with the other agents. The dissociation energy of the S-S bonds in different DPDS derivatives varies, as their environment influences their bonding strength. Walsh<sup>26</sup> pointed out the following four factors influencing the bond strength

- (i) Electronegative effects of the bonded groups
- (ii) Resonance effect
- (iii) Repulsion of filled atomic orbitals or steric effects
- (iv) Overlap of atomic orbitals, dependent on coplanarity of the phenyl-rings, allowing for full resonance.

Particularly in the *o*-substituted amine-derivatives, the resonance effect is the most important factor for aromatic compounds. This effect is shown in Figure 52. The number of possible resonance structures becomes smaller as R changes from C<sub>6</sub>H<sub>5</sub>CO- over CH<sub>3</sub>CO- to H- to none. When a C<sub>6</sub>H<sub>5</sub>CO- group sub-

stitutes R- in Figure 52, it results in a large corresponding resonance hybrid, allowing for very many resonance structures. Correspondingly, the resonance energy gain of the radical has the largest value with C<sub>6</sub>H<sub>5</sub>CO– as substituent. When the substituent is –NH<sub>2</sub>, the number of possible resonating structures is less and the resonance energy is also lower.

Steric hindrance and rotational strain may also have a serious effect on the strength of the disulfide bonds. If the substituent in an *o*-position is a bulky group, it is very unlikely that the molecule can take a coplanar configuration due to steric hindrance. The twisted molecule is stressed and therefore it breaks easier under formation of sulfidic radicals. C<sub>6</sub>H<sub>5</sub>CONH– is a bulkier group compared to –NH<sub>2</sub>, resulting in a stressed molecule, which releases the stress by making the molecule puckered and finally by breaking the –S–S– bond.

The observations described in the results section, can now be interpreted as follows

- (i) The rate constant of reclaiming increases with increasing temperature, for WLR1 as well as for WLR2. This is due to the fact that with increasing temperature the reactivity of the reclaiming agent's increases and the diffusion speed of the disulfide into the polymer matrix also rises, enhancing the chance of combination with a rubber radical. At higher temperatures, the polysulfides present in the rubber network are more easily broken.
- (ii) The rate constants of the reaction of WLR2 are in general higher than the constants for WLR1. On the other hand, the activation energy values for WLR2 are higher than for WLR1. A

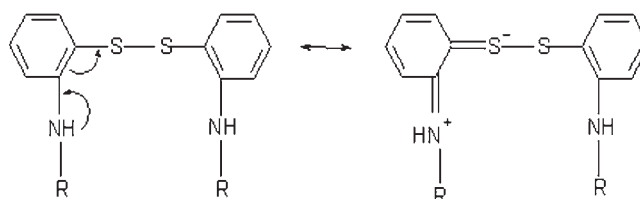


Figure 52 Resonance effect of amine *o*-substituted in general.

high activation energy signifies that the rate constant depends strongly on temperature. The network characterization of WLR1 and WLR2 was done and explained in detail in Table IV. The crosslink distribution of WLR2 and WLR1 done with thiol-amine method showed that WLR2 has 76%, and that WLR1 has 54% of polysulfidic crosslinks of the total crosslinks present in the two systems. Polysulfidic crosslinks are more temperature sensitive because they have the lowest bond energy of all the crosslinks present in the rubber network, Table I, and are easily broken. This explains the higher activation energy for WLR2.

A last point to mention is, that DBADPDS gives a significantly reduced smell during the reclamation process and of the final reclaim, relative to the other two agents, one of the most important shortcomings of the disulfides.

### CONCLUSIONS

A comparative study of DBADPDS with APDS and DPDS shows that DBADPDS is most reactive for the reclamation of NR based latex products, compared to the other aromatic disulfides studied. This is due to resonance and steric effects originating from the bulky benzamido-substituents on the *ortho*-position of the phenyl-rings, relative to the disulfidic bridge. Consequently, the disulfidic bridge of DBADPDS is more easily broken, so that it is able to break the crosslinks at temperature-levels  $\sim 20^\circ\text{C}$  below the temperature levels normally used in the reclamation process and necessary for the other two agents.

A main-chain to crosslink rupture study has shown, that all agents reclaim the vulcanizates mainly by crosslink scission. Analysis of the crosslink distribution using thiol-amine reagents has shown that all the poly- and disulfides are broken by DBADPDS. Mono-sulfides are not affected by neither of the aromatic disulfides chosen for the present study. The resonance energy of the radicals decrease in the order:

$\text{C}_6\text{H}_5\text{CONH—} > \text{CH}_3\text{CONH—} > \text{NH}_2\text{—}$ , corresponding to the ranking in reclamation efficiency of DBADPDS versus APDS

### References

1. Warner, W. C. *Rubber Chem Technol* 1994, 67, 559.
2. Yamashita, S. *Int Polym Sci Technol* 1981, 8, T/77.
3. Adhikari, B.; De, D.; Maiti, S. *Prog Polym Sci* 2000, 25, 909.
4. Isayev, A. I.; Chen, J.; Tukachinsky, A. *Rubber Chem Technol* 1995, 68, 267.
5. Levin, V. Y.; Kim, S. H.; Isayev, A. I. *Rubber Chem Technol* 1996, 69, 104.
6. Myhre, M. J.; MacKillop, D. A. *Rubber Chem Technol* 2002, 75, 429.
7. Novotny, D. S.; Marsh, R. L.; Masters, F. C.; Tally, D. N. (to Goodyear Tire and Rubber). U.S. Pat. 4,104,205 (1978).
8. Fix, S. R. *Elastomerics* 1980, 112, 38.
9. Onouchi, Y.; Inagaki, S.; Okamoto, H.; Furukawa, J. *Int Polym Sci Technol* 1982, 55, T/58.
10. Bateman, L. *The Chemistry and Physics of Rubber-like Substances*; Maclaren: London, 1963.
11. Hoover, F. I. Paper presented at the meeting of the Rubber Division, American Chemical Society, Pittsburg, October 8–11, 2002.
12. Verbruggen, M. A. L.; van der Does, L.; Noordermeer, J. W. M.; van Duin, M.; Manuel, H. J. *Rubber Chem Technol* 1999, 72, 731.
13. Dierkes, W.; Rajan, V.; Noordermeer, J. W. M. *Kautsch Gummi Kunstst* 2005, 58, 312.
14. Flory, P. J.; Rehner, J., Jr. *J Chem Phys* 1950, 18, 108.
15. Campbell, D. S. *J Appl Polym Sci* 1969, 13, 1201.
16. Campbell, D. S.; Saville, B. *Proceedings of the International Rubber Conference*, Brighton, UK, 1967; p 1.
17. Stafford, W. E.; Wright, R. A. *Rubber Chem Technol* 1958, 31, 599.
18. Horikx, M. M. *J Polym Sci* 1956, 19, 445.
19. Yashin, V. V.; Isayev, A. I. *Rubber Chem Technol* 1999, 72, 741.
20. Yashin, V. V.; Hong, C. K.; Isayev, A. I. *Rubber Chem Technol* 2004, 77, 50.
21. Kuan, T. H. *Rubber World* 1985, 192, 20.
22. Kok, C. M.; Yee, V. H. *Eur Polym Mater* 1986, 22, 341.
23. Imoto, M.; Kiriyaama, S. *Rubber Chem Technol* 1953, 26, 91.
24. Swain, C. G.; Stockmayer, W. H.; Clarke, J. T. *J Am Chem Soc* 1950, 72, 5426.
25. Blomquist, A. T.; Buselli, A. J. *J Am Chem Soc* 1951, 73, 3883.
26. Walsh, A. D. *J Chem Soc* 1948, 398, 27.